

## THE ORIGIN OF MERCURY'S SURFACE COMPOSITION, AN EXPERIMENTAL INVESTIGATION.

A. Boujibar<sup>1</sup>, K. Richter<sup>1</sup>, J. F. Rapp<sup>2</sup>, D. K. Ross<sup>2,3</sup>, K. M. Pando<sup>4</sup>, L. R. Danielson<sup>2</sup>, E. Fontaine, <sup>1</sup>NASA Johnson Space Center, Houston, TX 77058, <sup>2</sup>Jacobs, NASA Johnson Space Center, Houston, TX 77058, <sup>3</sup>UTEP-CASSMAR, El Paso TX 79968, <sup>4</sup>UTC– Jacobs JETS Contract, NASA Johnson Space Center, Houston, TX 77058.

**Introduction:** Results from MESSENGER spacecraft have confirmed the reduced nature of Mercury, based on its high core/mantle ratio and its FeO-poor and S-rich surface [1]. Moreover, high resolution images revealed large volcanic plains and abundant pyroclastic deposits [2], suggesting major melting stages of the Mercurian mantle. In addition, MESSENGER has provided the most precise data to date on major elemental compositions of Mercury's surface [3]. These results revealed considerable chemical heterogeneities that suggested several stages of differentiation and re-melting processes [4].

This interpretation was challenged by our experimental previous study, which showed a similar compositional variation in the melting products of enstatite chondrites, which are a possible Mercury analogue [5]. However, these experimental melts were obtained over a limited range of pressure (1 bar to 1 GPa) and were not compared to the most recent elemental maps [3]. Therefore, here we extend the experimental dataset to higher pressures and perform a more quantitative comparison with Mercury's surface compositions measured by MESSENGER. In particular, we test whether these chemical heterogeneities result from mixing between polybaric melts.

**Methods:** Experiments were conducted in a piston cylinder apparatus at NASA JSC at 0.5, 1 and 3 GPa and temperatures between 1250°C and 1880°C. The starting composition, similar to that used in [5], consisted of a mix of 50 wt% metal and 50 wt% silicate powders, with a chemical composition similar of EH4 enstatite chondrites. The starting metal was composed of 11 wt% S and 12 wt% Si. Experimental run products were analyzed with JEOL 8530F and Cameca SX100 electron micro-probes at NASA JSC. Oxygen fugacity ( $f_{O_2}$ ) was calculated in a similar manner to [5] and was between 2.9 and 4.8 log units below IW buffer.

**Results:** Phase proportions were determined by mass balance calculations. As with previous experiments performed at 1 GPa [5], new samples contain silicate melt, enstatite crystals and metal melt. Sulphide melts are also present in the majority of the samples.

Measured silicate melt compositions were compared with previous ones equilibrated at 1 GPa [5] and with a previously published study of EH4 chondrite melting at 1 bar [6]. Incompatible elements (Na, K and Al) decrease with the degree of melting (F), whereas com-

patible elements (Mg) increase with temperature. Major differences between chemical trends are for CaO and SiO<sub>2</sub>-contents. At low pressure and low F (1 bar and 0.5 GPa), the presence of Ca-rich sulfide induces a significant decrease of CaO-content in the silicate melt. On the other hand, the variation of silica-content differs with pressure. While it decreases with F at 1 bar, 0.5 and 1 GPa, it increases with F at 3 GPa. This is likely due to the fact that the bulk silicate composition has a Mg/Si molar ratio close to 1 (0.91 ± 0.04 for all samples). Enstatite melts incongruently and then congruently, below and above ~1 GPa, respectively, which changes the position of the eutectic point in the binary MgO-SiO<sub>2</sub> system. Hence, the concentration of silica decreases with F below ~1 GPa and increases with F above it.

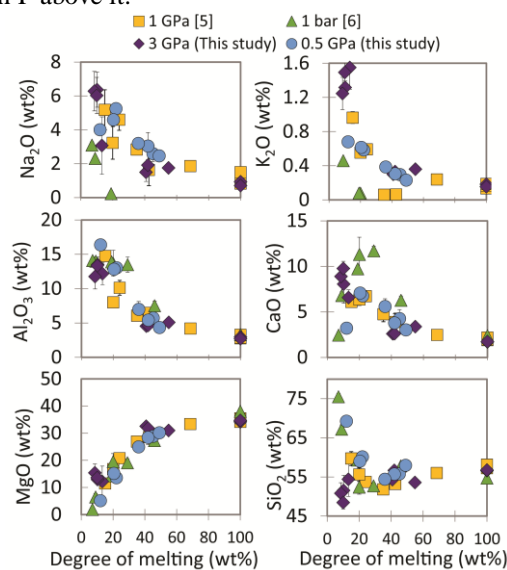


Figure 1: Chemical compositions of silicate melts as a function of the degree of melting. Our data are shown with those previously published [5-6].

To compare our data with Mercury's surface compositions, we quantitatively tested if the compositions generated by MESSENGER mapping result from mixing of two of the chemical compositions described by experimental trends. Based on published elemental ratios of Mercury's surface given in [3], we calculated normalized elemental concentrations of Mg, Ca, Si and Al ( $X_{\text{observed}}$  in the following). We also derived equations that predict the concentrations of Si, Mg, Al and Ca of experimental silicate melts (of this study and of [5-6]) as a function of the degree of melting for

each considered pressure (1 bar, 0.5, 1 and 3 GPa). We then tested if Mercury's compositions can match compositions resulting from mixing of two of these silicate melts ( $X_{\text{compo1}}$  and  $X_{\text{compo2}}$ ). This was performed using a linear regression where we investigated the fractions of each component ( $f_1$  and  $f_2=1-f_1$ ) by reducing the residue:

$$R^2 = [X_{\text{observed}} - X_{\text{calculated}}]^2 \quad (\text{eq.1})$$

where  $X_{\text{observed}} = f_1 * X_{\text{compo1}} + f_2 * X_{\text{compo2}}$  (eq.2)

Al/Si, Mg/Si and Ca/Si of experimental silicate melts from our study and that of [5-6] are compared with ratios of Mercury's surface in Fig. 2. Within the 730 Mercury compositions published in [3], we could resolve 592 using eq.1 against 138 compositions where no solution was found (Fig. 2). We applied the same calculation to the average geochemical provinces defined in [3]. All of these regions but the high-Al plains could be resolved from mixing of two components (Fig. 2). High-Al rich plains are therefore likely the result of several stages of differentiation and possibly melting of a feldspar-enriched source.

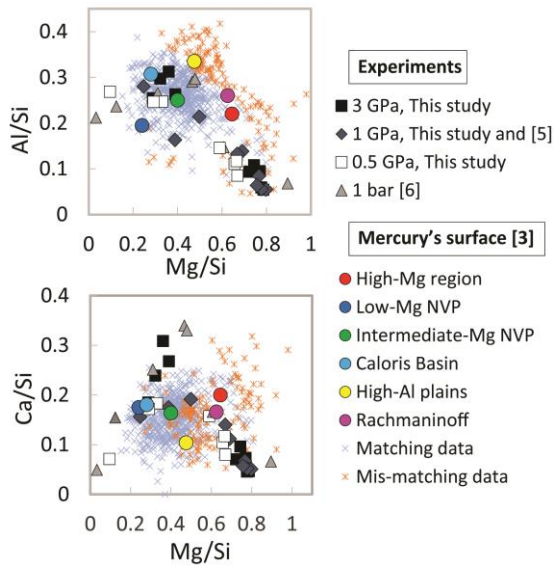


Figure 2: Comparison between Ca/Si, Al/Si and Mg/Si ratios of experimental silicate melts obtained in this study and that of [5-6] with Mercury's surface compositions (crosses: discrete compositions, and colored circles: average geochemical regions) [3]. Mercury's compositions that result in mixing of two of the melting products of enstatite chondrites are shown in blue while those where no solution is found are shown in red. NVP=North Volcanic Plains.

The resulting fractions of the two silicate melts whose mixing can match the compositions of Mercury's geochemical terranes are shown with their respective pressure and degree of melting in Table 1. The quality of the fit is illustrated in Fig. 3, showing that the model successfully reproduces the elemental ratios.

	Fract. compo 1	P (GPa)	F (wt%)	Fract. compo 2	P (GPa)	F (wt%)
High-Mg region	0.4	3	1	0.6	3	66
Low-Mg NVP	0.34	10 <sup>-4</sup>	1	0.11	10 <sup>-4</sup>	25
Int.-Mg NVP	0.89	3	19	0.66	1	1
Caloris Basin	0.78	3	12	0.22	1	1
Rachmaninoff	0.35	3	1	0.65	10 <sup>-4</sup>	69

Table 1: Result of the fitting model for resolvable Mercury's geochemical terranes. For each of them, fractions of the two melt components (Fract. Compo 1 and 2) and their respective pressure (P) and degree of melting (F) are shown.

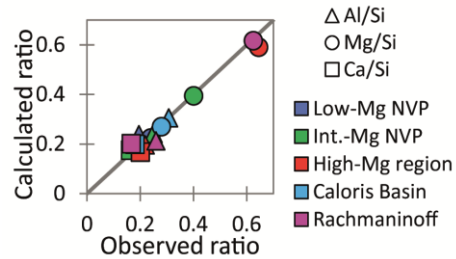


Figure 3: Comparison between the observed and calculated ratios of geochemical terranes using eq.2 (see text for more details).

Our experiments and models show that the majority of chemical diversity of Mercury's surface can result from melting of a primitive mantle compositionally similar to enstatite chondrites in composition at various depths and degrees of melting. The high-Mg region's composition is reproduced by melting at high pressure (3 GPa) (Tab. 1), which is consistent with previous interpretation as being a large degraded impact basin based on its low elevation and thin average crust [3]. While low-Mg NVP are the result of melting at low pressure (1 bar), intermediate-Mg NVP, Caloris Basin and Rachmaninoff result from mixing of a high-pressure (3 GPa) and low-pressure components (1 bar for Rachmaninoff and 1 GPa for the other regions) (Tab. 1). Moreover, all compositions suggest mixing between low and high degree melts that indicate important differentiation processes.

**References:** [1] Zolotov M. Y. et al. (2013) *JGR*, 118, 138-146. [2] Solomon S. C. et al. (2011) *Planet Space Sci.*, 59, 1827-1828. [3] Weider et al. (2015) *EPSL*, 416, 109-120. [4] Charlier B. et al. (2013) *Earth & Planet. Sci. Let.* 363, 50-60. [5] Boujibar et al. (2014) *46<sup>th</sup> LPSC*, Abstract #2544. [6] McCoy T. J. et al. (1999) *Meteoritics & Planet. Sci.*, 34, 735-746.